

## Electronic Supplementary Information

### Oxide rupture-induced conductivity in liquid metal nanoparticles by laser and thermal sintering

Shanliangzi Liu, Serrae R. Reed, Matthew J. Higgins, Michael S. Titus, and Rebecca Kramer-Bottiglio\*

#### List of Contents

Table S1. The list of selected and calculated laser sintering parameters: average power, pulse repetition rate, pulse energy and fluence

Table S2. The list of laser speed and pulse spacing at varying pulse overlap and a fixed pulse repetition rate (200 kHz)

Fig. S1. SEM image of laser sintered liquid nanoparticle film ( $3.11 \text{ J/cm}^2$ , 50%) after scratch test

Fig. S2. SEM image of thermal sintered liquid nanoparticle film ( $500^\circ\text{C}$ ) after scratch test

Fig. S3. SEM image of liquid metal nanoparticle film thermally sintered at  $500^\circ\text{C}$

Fig. S4. EDS analysis of thermal sintered liquid metal nanoparticle film at  $600^\circ\text{C}$

Fig. S5. EDS analysis of thermal sintered liquid metal nanoparticle film at  $800^\circ\text{C}$

Fig. S6. Observation of the brighter clusters appeared at  $800^\circ\text{C}$  after heating up to  $900^\circ\text{C}$  for different time durations

Fig. S7. HAADF STEM image and corresponding EDS analysis of a single nanowire separated from thermal sintered liquid metal nanoparticle film at  $900^\circ\text{C}$

Fig. S8. Nanowire growth at  $800^\circ\text{C}$  and  $900^\circ\text{C}$  for only 5 minutes

Fig. S9. Surface morphology of thermal sintered liquid metal nanoparticle film at  $900^\circ\text{C}$  for 12 hrs

Fig. S10. Cross-section images of as-printed and laser sintered liquid metal nanoparticles at  $4.4 \text{ J/cm}^2$ , 40% and  $4.4 \text{ J/cm}^2$ , 80%

Fig. S11. X-ray diffraction pattern of thermal sintered liquid metal nanoparticle film at  $900^\circ\text{C}$  for 12 hrs

Fig. S12. Ga 2p XPS core level spectra of liquid metal nanoparticle films sintered at varying laser parameters and heating temperatures

#### Laser Sintering Parameters

Laser fluence and beam pulse overlap were varied to study the effect of laser energy on liquid metal nanoparticle films. Laser fluence is defined as optical energy delivered per unit area:

$$F[\text{J/cm}^2] = \frac{E}{\frac{1}{4}\pi s^2} \quad (1)$$

where  $E$  is laser pulse energy (J/pulse) and  $s$  is laser spot size ( $\mu\text{m}$ ).

Beam pulse overlap is defined as the percentage amount of overlap between the diameters of two consecutive pulses:

$$O[\%] = \left[1 - \frac{v}{fs}\right] \times 100\% \quad (2)$$

where  $v$  is laser scanning speed (mm/s) and  $f$  is pulse repetition rate (kHz). Here, the laser spot size is a theoretical value. The actual beam spot size should increase with laser power and decrease with laser scanning speed.

In addition, laser average power is defined as

$$P[\text{W}] = Ef \quad (3)$$

The selected and calculated laser parameters are listed in the tables below:

**Table S1** The list of selected and calculated laser sintering parameters: average power, pulse repetition rate, pulse energy and fluence.

Average Power (W)	Pulse Repetition Rate (kHz)	Pulse Energy (mJ/pulse)	Fluence ( $\text{J}/\text{cm}^2$ )
0.7	260	0.00269	1.52
0.8	240	0.00333	1.89
0.9	220	0.00409	2.31
1.1	200	0.00550	3.11
1.4	180	0.00778	4.4
1.7	160	0.01063	6.01
2.1	140	0.01500	8.49

**Table S2** The list of laser speed and pulse spacing at varying pulse overlap and a fixed pulse repetition rate (200 kHz).

Pulse Repetition Rate (kHz)	Laser Speed (mm/s)	Pulse Overlap (%)	Pulse Spacing ( $\mu\text{m}$ )
200	1800	40	9
200	1500	50	7.5
200	1200	60	6
200	900	70	4.5
200	600	80	3
200	300	90	1.5

## Supplemental Figures

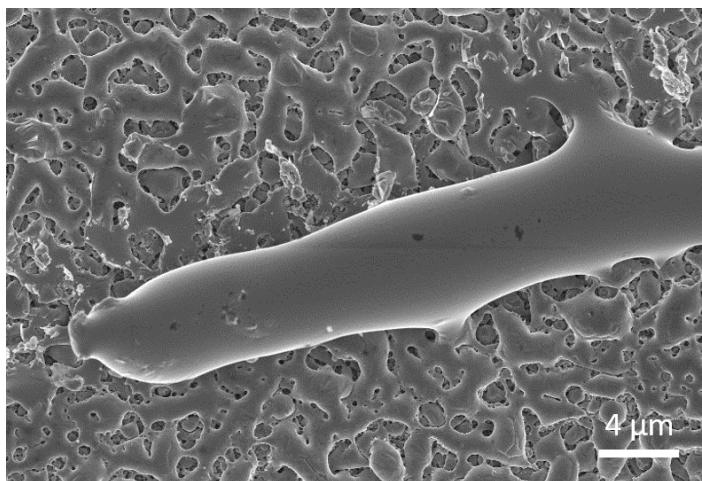


**Fig. S1** SEM image of laser sintered liquid nanoparticle film ( $3.11 \text{ J}/\text{cm}^2$ , 50%) after scratch test. The oxide breaks and the laser coalesced network reflows into a complete liquid trace.

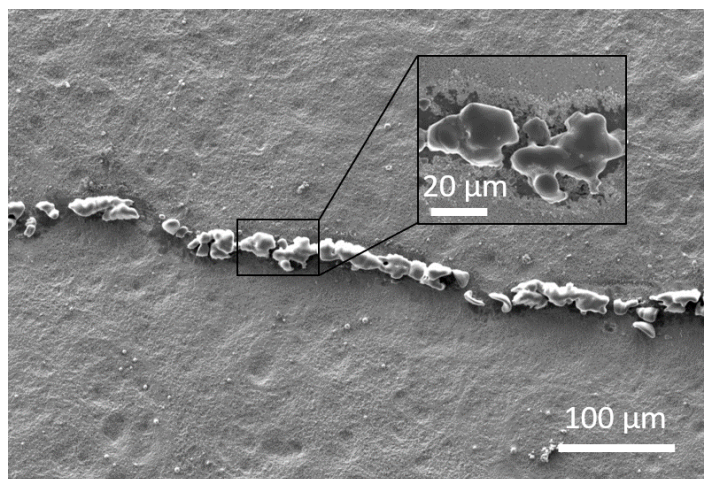


**Fig. S2 SEM image of thermal sintered liquid nanoparticle film (500 °C) after scratch test.** The liquid trace is not fully continuous, indicating that the amount of liquid left in the cores is small due to large oxidation.

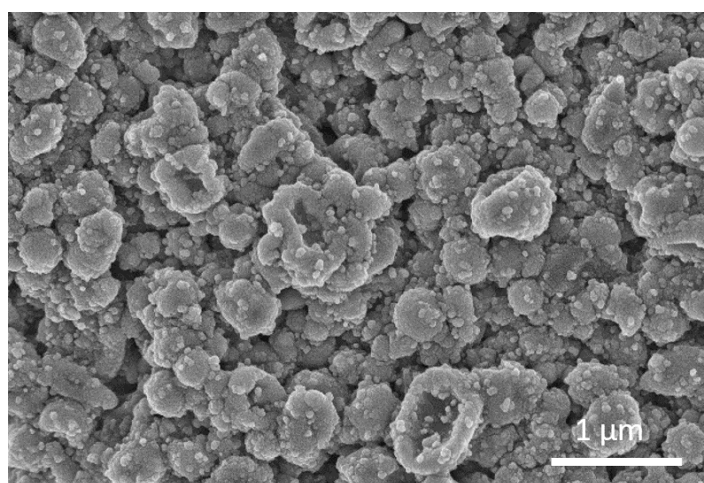


**Fig. S3 SEM image of liquid metal nanoparticle film thermally sintered at 500 °C.** The small brighter nanoparticles are well distributed over the entire surface of the film.

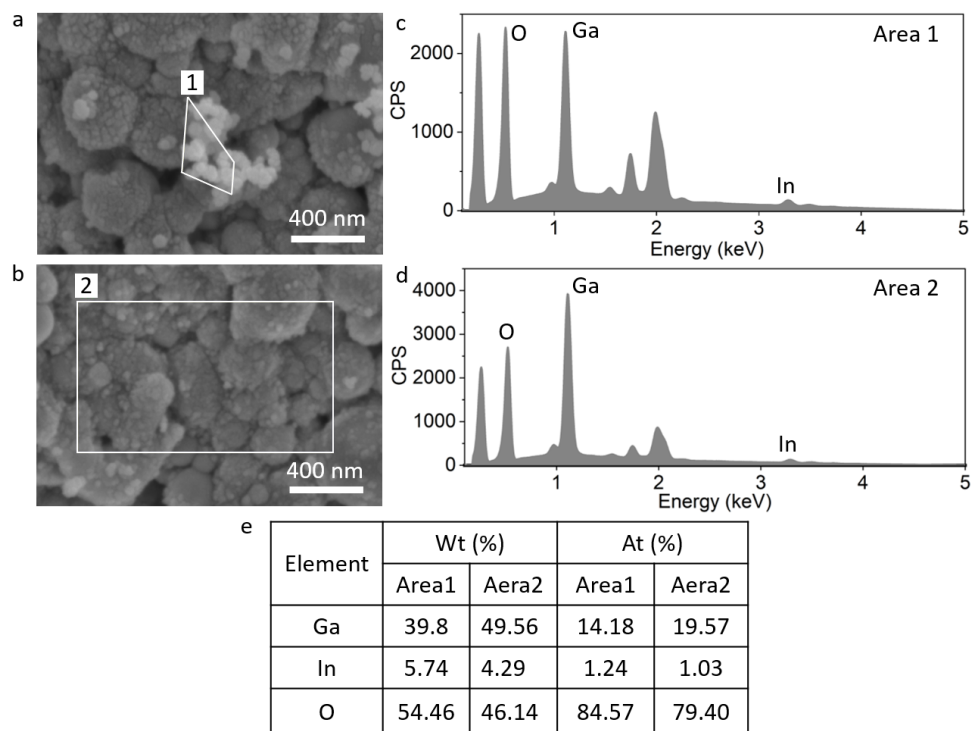


**Fig. S4 EDS analysis of thermal sintered liquid metal nanoparticle film at 600 °C.** (a-b) SEM images of selected areas with (1) or without (2) brighter nanoparticle clusters. (c-e) EDS spectra and calculated mass/atomic percentage of the two selected areas. The results show that the region with the brighter nanoparticle clusters is more oxidized and has a higher content of indium.

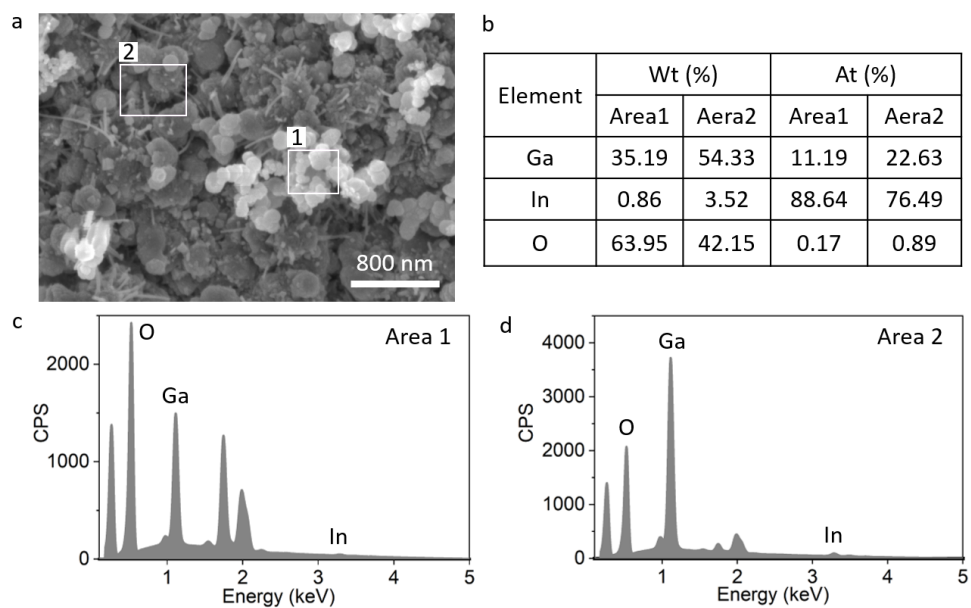


**Fig. S5 EDS analysis of thermal sintered liquid metal nanoparticle film at 800 °C.** (a) SEM image of selected areas with (1) or without (2) big clusters. (b-d) Calculated mass/atomic percentage and EDS spectra of the two selected areas. The results show that the region with the big brighter clusters is highly oxidized.

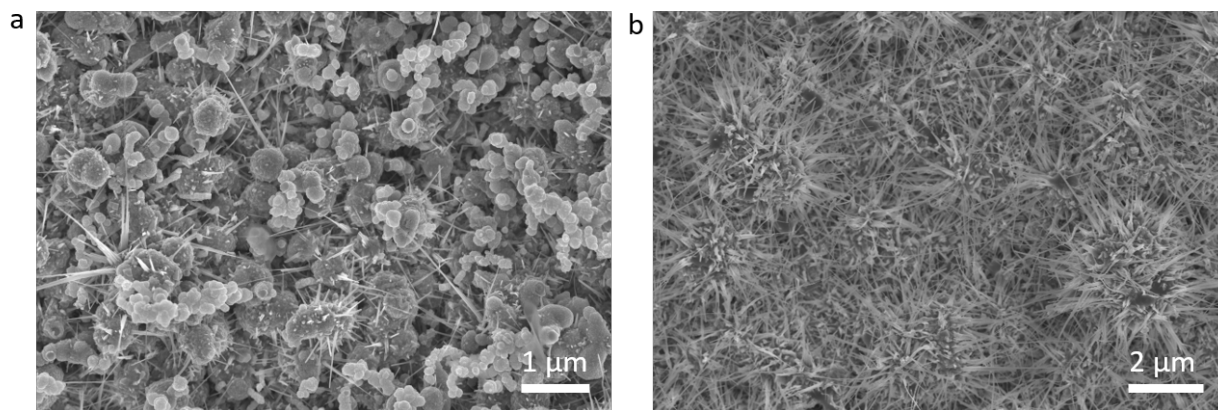


**Fig. S6 Observation of the brighter clusters appeared at 800 °C after heating up to 900 °C for different time durations.** Liquid metal nanoparticle film thermally sintered at 800 °C was heated up to 900 °C from room temperature for 30 min (a) and 5 hrs (b). In (a), the brighter clusters are still present, and more nanowires appear. In (b), all the brighter clusters are gone and nanowires are grown extensively, covering the entire surface. The brighter clusters likely grow into facets or fall off the surface.

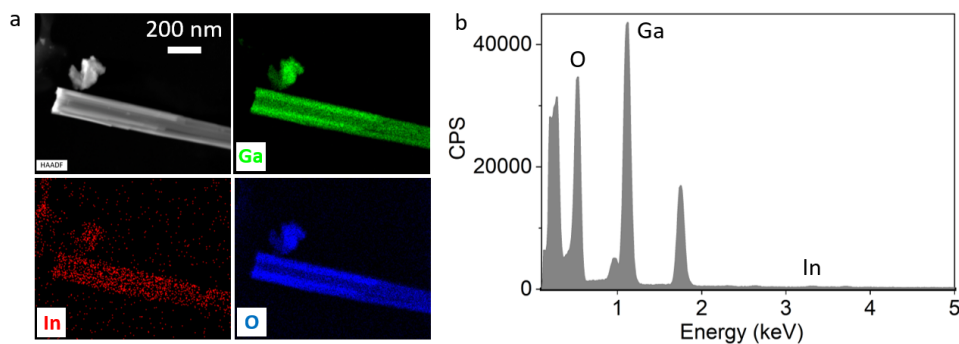


**Fig. S7 HAADF STEM image and corresponding EDS analysis of a single nanowire separated from thermal sintered liquid metal nanoparticle film at 900 °C.** Single nanowires were separated from the particles by sonicating in isopropyl alcohol for a few minutes and then drop casted onto a copper grid for imaging. (a) HAADF STEM image and Ga, In, O elemental mappings. (b) EDS spectrum of the nanowire. The results demonstrate that the nanowires are primarily composed of Ga and O, with a negligible amount of In.

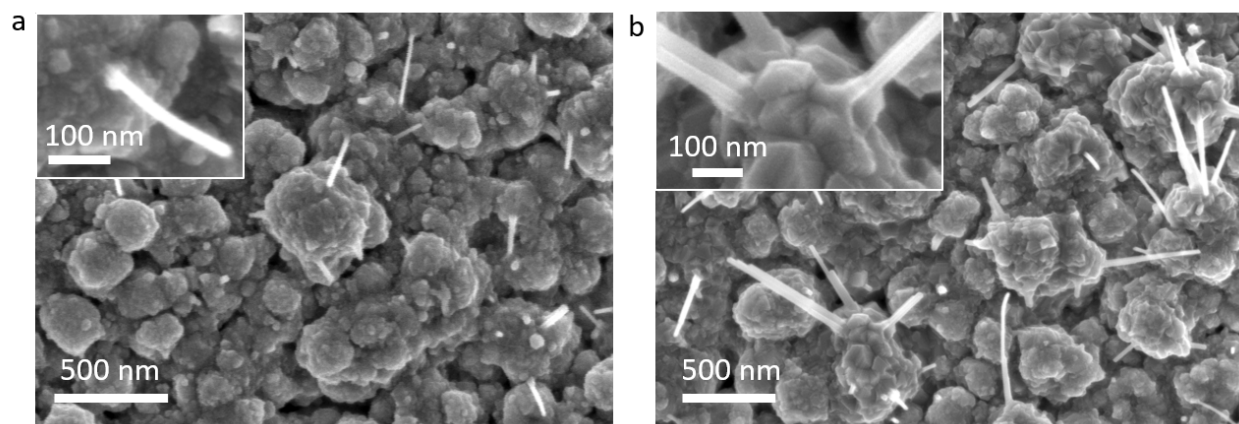


**Fig. S8 Nanowire growth at 800 °C and 900 °C for only 5 minutes.** (a) At 800 °C, nanowires are grown out of brighter nanoparticles on the parent particles. (b) At 900 °C, the surface of the film is significantly oxidized and crystallized. Nanowires are nucleated from the facets.



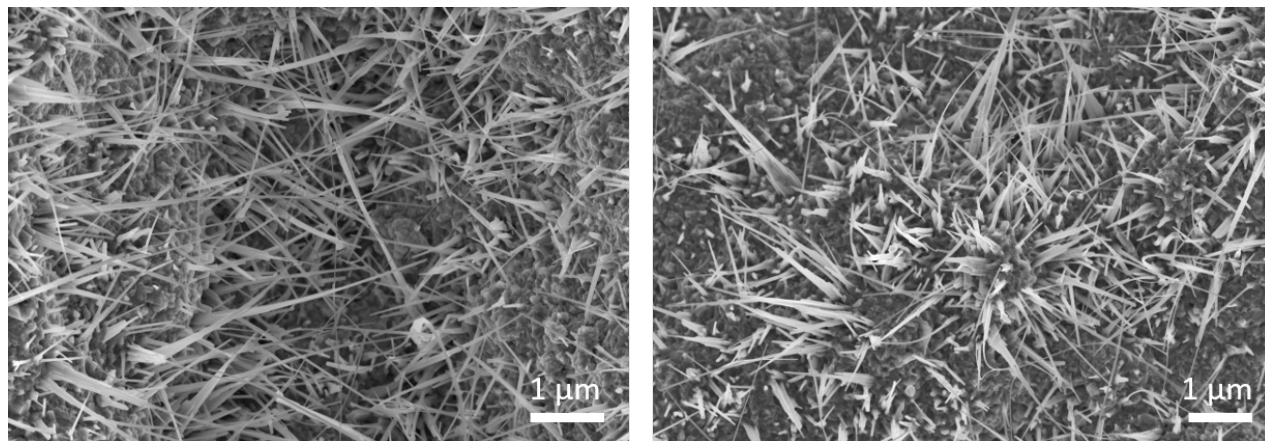


**Fig. S9** Surface morphology of thermal sintered liquid metal nanoparticle film at 900 °C for 12 hrs. The density and lengths of nanowires are significantly increased.

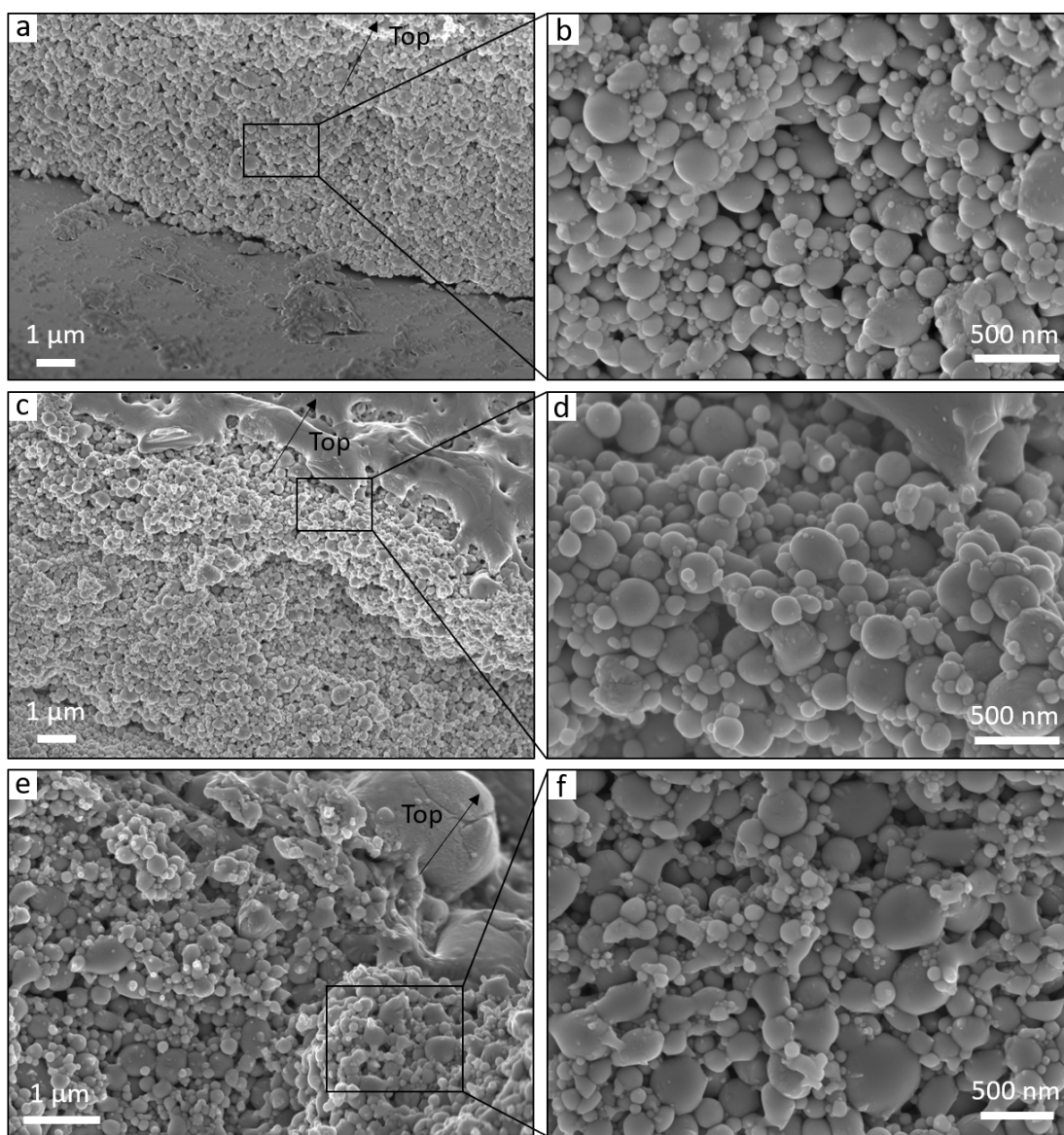


**Fig. S10** Cross-section images of as-printed liquid metal nanoparticles (a-b) and laser sintered nanoparticles at 4.4 J/cm<sup>2</sup>, 40% (c-d) and 4.4 J/cm<sup>2</sup>, 80% (e-f). The uncoalesced particles underneath the top coalesced regions of the laser sintered samples are more closely packed maybe due to partial sintering from the instantaneous heating of the laser beam.

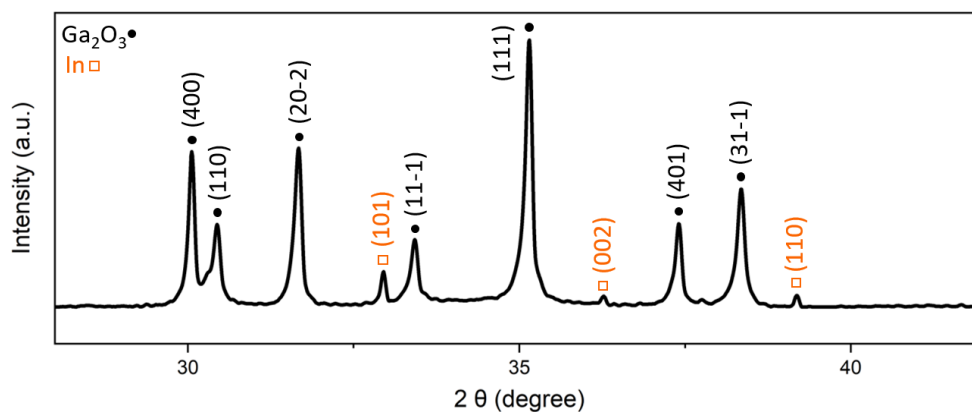


**Fig. S11 X-ray diffraction pattern of thermal sintered liquid metal nanoparticle film at 900 °C for 12 hrs.** The identified diffraction peaks correspond to tetragonal indium (orange, space group  $I4/mmm$ , PDF #00-005-0642) and monoclinic  $\beta$ -Ga<sub>2</sub>O<sub>3</sub> (black, space group  $C2/m$ , PDF #01-087-1901).

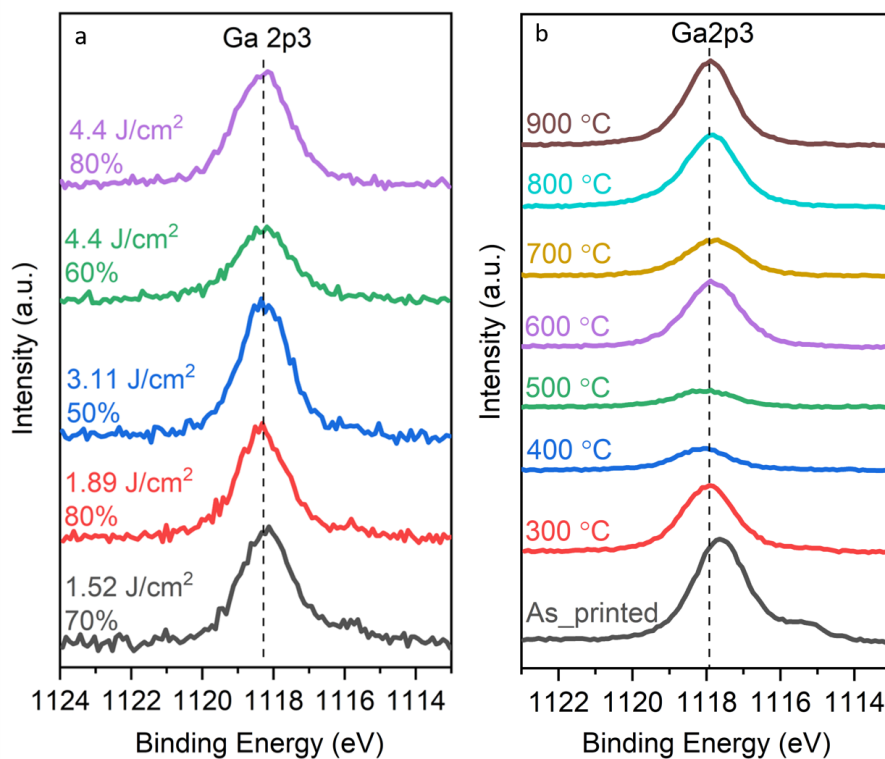


**Fig. S12 Ga 2p XPS core level spectra of liquid metal nanoparticle films sintered at varying laser parameters (a) and heating temperatures (b).**